Fuel 309 (2022) 122032

Contents lists available at ScienceDirect

Fuel

journal homepage: www.elsevier.com/locate/fuel

Scrutinizing proposed extensions to the Eddy Dissipation Concept (EDC) at low turbulence Reynolds numbers and low Damköhler numbers

Ivar S. Ertesvåg

Department of Energy and Process Engineering, NTNU Norwegian University of Science and Technology, Kolbjørn Hejes vei 1b, NO 7491, Trondheim, Norway

ARTICLE INFO

Keywords:
Turbulence
Combustion
Modeling
Cascade
Magnussen's EDC
Parente's extension
Extended EDC

ABSTRACT

Recent proposals to modify or extend the Eddy Dissipation Concept are investigated and compared to the standard EDC. The results with respect to the underlying principles of EDC are examined. A total of four different variants of the extended EDC are available, expressing locally determined values for two model coefficients that are constants in the standard EDC. The effects on the fine-structure region mass fraction and the fine structure time scale are demonstrated with resulting effects on the mixing and species mean reaction rate. It is found that the constraints imposed on the locally determined coefficients are more important for the results than the formulated dependencies of turbulence Reynolds number and microscale Damköhler number. Furthermore, some of the versions require a less-than-unity limitation for the fine-structure mass fraction for wide ranges of the Reynolds number. All the modified model versions maintain the EDC cascade model, and their relations to this model are investigated. A finding is that some versions maintain very high viscous effects at high turbulence Reynolds numbers. Comparison with the standard EDC shows that some of the effects motivating the extensions are already present in the standard EDC. Initially, a short cascade for low turbulence Reynolds numbers is derived from the existing EDC cascade model, which was developed for high Reynolds numbers. The resulting changes are small, and the need for a modification still remains.

1. Introduction

The Eddy Dissipation Concept for turbulent combustion (EDC) was proposed 40 years ago by Magnussen [1]. With modest changes, it has been applied by engineers and scientists and validated against a wide range of experimental data. It has been used with a variety of two- and multi-equation Reynolds-averaged Navier–Stokes (RANS) turbulence models and with large-eddy simulations (LES). The chemistry models used in conjunction with EDC ranges from simple, infinitely fast global reactions to full kinetic mechanisms. In recent years it has become known as a model capable of handling MILD (Moderate or Intense Low-oxygen Dilution) combustion, however with some drawbacks. This has led to a multitude of simple adjustment of numerical coefficients, as reviewed and analyzed previously [2].

Parente and co-workers [3,4] suggested to modify or extend EDC such that the turbulence Reynolds number and the small-scale Damköhler number are included in the expressions reactor time scale, the fine-structure mass fraction and, consequently, the reaction rate. This was motivated by some observed challenges regarding MILD combustion. This regime is characterized by distributed reactions. Besides the MILD regime, relevant for energy-conversion purposes, also enclosed fires possess some of the same features, as weakened turbulence and low-oxygen reactions.

Lewandowski et al. [5] suggested a variant of the extended model. Another amendment of Parente's model was initially made by Bao [6], with a follow-up by Romero-Anton et al. [7]. They arrived a slightly different version of the modifications. A third amendment was proposed recently by Fordoei et al. [8].

A central idea of EDC is that chemical reactions occur in fine structures or small eddies of turbulence [1]. Here, the local gradients of species and temperature are large, providing good local mixing. At the same locations, the velocity gradients, hence the turbulence energy dissipation, are large. Thus, the chemical reactions mainly occur where the dissipation mainly occurs.

Main parts of EDC are a turbulence energy cascade model, a reactor model and the interactions between these. The cascade connects the reacting fine structures to the mean flow and mixing, which are described by a turbulence model, e.g., a k-ε model or a Reynolds-stress equation model.

Input to the cascade model is the turbulence energy and its dissipation rate, provided by the chosen turbulence model. The output of the cascade is the scales of the fine structures, that is, length, velocity and time representing the small eddies. The reactor model describes the local reactions in the fine structures and provide an expression for the

E-mail address: Ivar.S.Ertesvag@ntnu.no.

https://doi.org/10.1016/j.fuel.2021.122032
Received 1 May 2021; Received in revised form 14 July 2021; Accepted 15 September 2021

mean reaction rate. This is the source term of the mean species mass balance. In the reactor, the chemical reactions can be formulated as a single-step or multistep chemical mechanism. The reactor can be in the form of a homogeneous open reactor (transient or steady-state well stirred reactor), or a batch reactor. Other forms of reactors might be feasible.

The cited proposals to extend EDC act partly to modify quantities of the cascade and partly to modify the cascade-reactor interaction expressions.

The aims of the present work are to examine the proposed modifications, explore the effects of weak turbulence or low turbulence Reynolds numbers on EDC, and to discuss possible developments to improve modeling in this regime. In the first place, Section 2, the original expressions of EDC will be reviewed. The EDC cascade model was originally developed for high turbulence Reynolds numbers, that is, with a large number of cascade levels. Here, in Section 3, a short version of the cascade will be developed. This has not been done previously and seems as a natural first step before exploring the proposed low-Reynolds number modifications. Subsequently, in Section 4 the modifications of Parente and co-workers [3–5] will be reviewed and examined. The related modifications by Bao [6], Romero-Anton et al. [7] and Fordoei et al. [8] will also be included. Investigations by said authors have been made by comparison to one or more sets of flame experimental data. Contrary to those, the present work will discuss the modified models from the principles of EDC. That is, compare the key quantities constituting the cascade, reactor and mean reaction rate of EDC. Both the proposals and the present investigation are made in a RANS context, although some aspects are relevant for LES.

Finally, the overall discussion and conclusions are summarized in the two last sections.

2. Turbulence and turbulence-chemistry interactions with EDC

2.1. Scales of turbulence

The turbulent flow is modeled with some turbulence model. Most of the available two-equation models and Reynolds-stress-equation models provide quantities like the turbulence energy, k, and its dissipation rate, ε. From these, scales for velocity, $k^{1/2}$, length, $k^{3/2}/\varepsilon$, and time, k/ε, can be expressed, together with a turbulence viscosity, ν_t. The corresponding turbulence Reynolds number Re_T can be defined as

$$Re_T = \frac{k^2}{\nu\varepsilon}. \tag{1}$$

These scales are "large" scales, that is, representing the effects of large/medium size eddies and diffusive mixing due to turbulence.

The "small" scales of turbulence, the Kolmogorov scales for length, velocity and time, are expressed as

$$\eta = \left(\frac{\nu^3}{\varepsilon}\right)^{1/4}, \quad v_\eta = (\nu\varepsilon)^{1/4} \quad \text{and} \quad \tau_\eta = \left(\frac{\nu}{\varepsilon}\right)^{1/2}. \tag{2}$$

At instances with low production of turbulence, the eddying motions will become weaker. The turbulence energy and its dissipation rate will decline, and so also the turbulence Reynolds number. The "large" time scales will increase, and if external constraints allow, so also the "large" length scales.

2.2. Damköhler number

The microscale Damköhler number can be defined as $Da_\eta = \tau_\eta/\tau_c$, where τ_c is a chemical time scale. The microscale Damköhler number relates to the macroscale Damköhler number as $Da_\theta = (k/\varepsilon)/\tau_c = Da_\eta \cdot Re_T^{1/2}$.

Determining the chemical timescale can be a challenge by itself. This is out of scope of the current work. It will be assumed that a chemical time scale can be determined and hence, a Damköhler number.

2.3. Low and high Damköhler and Reynolds numbers

Terms like "low" and "high", about Damköhler and Reynolds numbers, are often met in literature; also "approaching" or "close to" unity, about Damköhler numbers. The precise quantification can be less clear. Moreover, the definitions can be diverse.

Most prominently, there are two different Damköhler numbers; microscale and macroscale, cf. Section 2.2 above. Furthermore, how to define and practically calculate the chemical time scale involved, is the subject of discussions in literature. There is some variation in the definitions of the turbulence Reynolds number, as well. Modelers often prefer $k^2/(\nu\varepsilon)$ (Eq. (1)), since the involved quantities are readily available from a turbulence model. Experimentalists may prefer other definitions.

To illustrate the ranges of the parameters, Table 1 shows exemplary data from literature.

2.4. Review of some Eddy dissipation cascade and reaction rate expressions

The cascade model was described in detail in [16,17] and originally presented by Magnussen (1981,1989) [1,18]. Some related aspects of the model were also discussed in [2]. The development and basic considerations are not repeated. For convenience and discussion, some resulting expressions are shown here.

The cascade model [17] leads to the expressions

$$\varepsilon = 2C_{D1}\frac{u^{*3}}{L^*} \tag{3}$$

and

$$\varepsilon = \frac{4}{3}C_{D2}\nu\frac{u^{*2}}{L^{*2}}. \tag{4}$$

Combining these, the fine-structure length and velocity scales are developed as

$$L^* = \frac{2}{3}\left(\frac{3C_{D2}^3}{C_{D1}^2}\right)^{1/4}\left(\frac{\nu^3}{\varepsilon}\right)^{1/4} = \left(\frac{2^3}{3}\right)^{1/2} C_\tau C_\gamma \left(\frac{\nu^3}{\varepsilon}\right)^{1/4} \tag{5}$$

and

$$u^* = \left(\frac{C_{D2}}{3C_{D1}^2}\right)^{1/4}(\nu\varepsilon)^{1/4} = \left(\frac{2}{3}\right)^{1/2} C_\gamma(\nu\varepsilon)^{1/4}. \tag{6}$$

Here, the secondary constants C_γ and C_τ are introduced from Eqs. (10) and (11) below. The scales L^* and u^* are of the same order of magnitude as the Kolmogorov scales (Eq. (2)), which are seen as factors in the expressions. The corresponding Reynolds number becomes

$$Re^* = \frac{u^* L^*}{\nu} = \frac{2C_{D2}}{3C_{D1}} = \frac{4}{3}C_\tau C_\gamma^2. \tag{7}$$

The EDC cascade model can be viewed as a dissipation model with an inertial term and a viscous term [1,2,17],

$$\varepsilon = \varepsilon_1 + \varepsilon_2 = C_{D1}\omega k + C_{D2}\nu\omega^2. \tag{8}$$

The ratio of the viscous term to the total dissipation rate can be expressed as

$$\frac{\varepsilon_2}{\varepsilon} = \left(1 + Re_T\frac{C_{D1}^2}{2C_{D2}}\right) - \left(\left(1 + Re_T\frac{C_{D1}^2}{2C_{D2}}\right)^2 - 1\right)^{1/2}, \tag{9}$$

where $C_{D1}^2/(2C_{D2}) = 3/(8C_\gamma^4)$ can be introduced. It was shown [2] that the EDC standard constants gave results close to those of the constants recommended by [19] from experiments and DNS.

Table 1
Data examples from literature; type and source of data; ranges of Damköhler and Reynolds numbers.

Reference	Type	Da_η	Re_T	Comment
Skiba et al. [9]	Review, premixed, DNS	0.001–1	1–10^2	
	Review, premixed, experiments	0.0003–3	10–10^3	
	Experiments	0.001–1	10^2–10^4	"Extreme levels of turbulence" intended
Savre et al. [10]	2-d DNS, premixed	~0.01	16–103	
Lewandowski [5,11]	MILD, review and own RANS computations	0–3	0–200	Delft and Adelaide Jet-in-hot coflow
Li et al. [12]	Experiments, MILD	0.0003–1	10^2–10^3	
Minamoto et al. [13,14]	DNS, MILD	0.08–0.5	67–96	
	DNS, premixed	~1.1	~38	
Sorrentino et al. [15]	Experiments, MILD			Da_θ~0.1–1

2.5. EDC cascade-reactor interaction quantities

EDC provides the expressions for the fine-structure region mass fraction,

$$\gamma_\lambda = \left(\frac{3C_{D2}}{4C_{D1}^2}\right)^{1/4}\left(\frac{\nu\varepsilon}{k^2}\right)^{1/4} = C_\gamma\, Re_T^{-1/4}, \tag{10}$$

and the fine-structure time scale,

$$\tau^* = (\dot{m}^*)^{-1} = \left(\frac{C_{D2}}{3}\right)^{1/2}\left(\frac{\nu}{\varepsilon}\right)^{1/2} = C_\tau\left(\frac{\nu}{\varepsilon}\right)^{1/2}, \tag{11}$$

where the secondary, single-symbol constants C_γ and C_τ are introduced for convenience and discussion. The Kolmogorov time scale is recognized in the variable factor of Eq. (11). Reverting the expressions, the primary constants can be expressed as $C_{D1} = 3C_\tau/(2C_\gamma^2)$ and $C_{D2} = 3C_\tau^2$. From the cascade model can also be expressed $L^*/L' = (4/3)\gamma_\lambda^3$. Here, L' is the large length scale of turbulence, corresponding to the Prandtl mixing length.

The mean reaction rate contains the quantity γ_λ^2/τ^*, which can be expressed as

$$\frac{\gamma_\lambda^2}{\tau^*} = \frac{3}{2C_{D1}}\frac{\varepsilon}{k} = C_R\frac{\varepsilon}{k} = \frac{C_\gamma^2}{C_\tau}\frac{\varepsilon}{k}. \tag{12}$$

In the 2nd equality here, the symbol C_R was introduced for $(3/(2C_{D1}))$, and in the third equality, the constants C_γ and C_τ from Eqs. (10) and (11) were used.

With the standard values of the primary constants, $C_{D1} = 0.135$ and $C_{D2} = 0.50$ [17], the fine-structure Reynolds number becomes $Re^* = 2.47$, and the secondary constants take the values $C_\gamma = 2.130$, $C_\tau = 0.4082$ and $C_R = 11.1$.

The EDC mean reaction rate is expressed as

$$\overline{R}_k = \frac{\chi\gamma_\lambda^2\bar{\rho}}{\tau^*(1-\chi\gamma_\lambda^n)}\left(Y_k^* - \widetilde{Y}_k\right), \tag{13}$$

where $\widetilde{Y}_k$ and Y_k^* are, respectively, the mean and fine-structure reactor mass fractions of the species. In 1989, Magnussen [18,20] set $n = 3$, whereas the original $n = 2$ ([1], with γ_λ^{-1} included within χ) was reintroduced in 2005[21]. The latter value is recommended.

The fraction χ appearing in Eq. (13) describes the fraction of the fine structures that are reacting. It is composed [20] of factors $\chi = \chi_1\chi_2\chi_3$, which can be reformulated [2] as

$$\chi_1 = \min\{\lambda^{-1}, \lambda\}, \tag{14}$$

$$\chi_2 = \min\left\{(c/\gamma_\lambda), 1\right\} \tag{15}$$

$$\chi_3 = \min\left\{\gamma_\lambda/(1-c), 1\right\}, \tag{16}$$

where λ is the air excess ratio (reciprocal of the equivalence ratio), and c is a reaction progress variable, both evaluated for the local mean composition,

$$\lambda = \frac{\widetilde{Y}_{ox}/r + \widetilde{Y}_{pr}/(1+r)}{\widetilde{Y}_{fu} + \widetilde{Y}_{pr}/(1+r)}, \tag{17}$$

$$c = \frac{\widetilde{Y}_{pr}/(1+r)}{\min\{\widetilde{Y}_{fu}, \widetilde{Y}_{ox}/r\} + \widetilde{Y}_{pr}/(1+r)}. \tag{18}$$

Here, "fu", "ox" and "pr" denote, respectively, fuel, oxidizer and product of a one-step global reaction, and r is the stoichiometric mass-based oxidizer requirement of the fuel. The factor χ_1 describes the coincidence of fuel and oxidizer, χ_2 describes the extent of heating, while χ_3 limits the reaction due to lack of reactants [20].

Gran [20] suggested $\chi = 1$ as a possible simplification, which has been applied by several investigators. It was, however, shown [22] that a less-than-unity χ can be significant.

In the following, "standard EDC" will denote use of Eq. (13) with $n = 2$, χ from Eqs. (14)–(16), and Eqs. (5)–(6) and (11)–(12) with $C_{D1} = 0.135$ and $C_{D2} = 0.50$.

2.6. Fine structures, limiting considerations

In literature, some claims exist that the EDC fine-structure reactor model is limited to $Re_T > 65$, with the associated limitation $\gamma_\lambda < 0.75$. As shown [2], these claims were based on a misunderstanding and are valid only for a special implementation of EDC into Ansys Fluent, not for EDC in general.

The ratio of mass in fine-structure regions to the total mass, γ_λ, is expressed by Eq. (10). A trivial limit for this expression is seen from the condition $\gamma_\lambda < 1$. Then, with the standard constants, $Re_T > 20.6$. At lower values of Re_T, γ_λ becomes larger than unity, and the denominator $(1 - \chi\gamma_\lambda^2)$ might become negative (depending on χ). Alternatively, the expression for γ_λ can be modified, as attempted by Myhrvold [23] (pp. 95–104).

Practically, an upper limit has been imposed on γ_λ. The limit has been set somewhat arbitrary by various investigators to 0.7–0.9. The limit is often not reported, perhaps not even known, by the users. For instance, the theory and user's guides [24,25] of the widely used CFD code Fluent do not mention a limiting value.

The ratio of the fine-structure timescale, Eq. (11), to the turnover timescale k/ε can be expressed as

$$\frac{\tau^*}{k/\varepsilon} = C_\tau\left(\frac{\nu\varepsilon}{k^2}\right)^{1/2} = C_\tau Re_T^{-1/2}. \tag{19}$$

Since the fine-structure exchange occurs locally, inside the overall volume, it is reasonable to require this ratio to be less than unity. The limit is reached at $Re_T = C_\tau^2$, which for the standard constants means $Re_T = 0.17$.

A third issue to note is that the EDC cascade model was developed [17] with the assumption of high turbulence Reynolds number, that is, with many levels in the cascade. The exact implications of this assumption have not previously been investigated.

These considerations show improvement potentials for EDC at low Re_T. They do not exclude the possibilities of other reasons for modifications of the model, with effects also at higher values of Re_T.

For the context, it can be noted that for the standard k-ε model [26], and also for the k-ω^2 and k-ω models by Saffman and Wilcox [27,28], the ratio of turbulence viscosity to molecular viscosity can be expressed

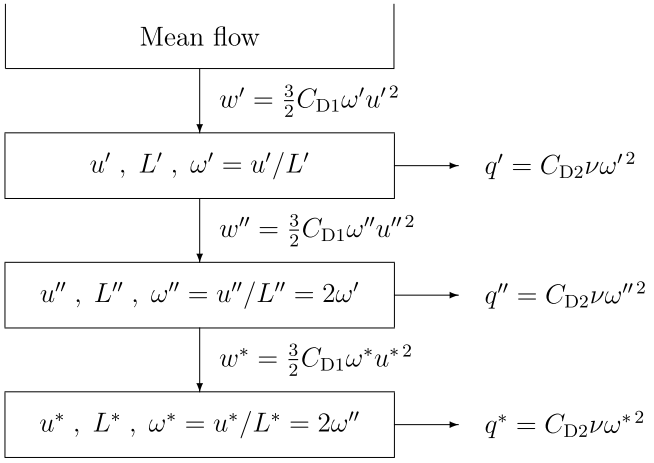

Fig. 1. Three-level EDC turbulence energy cascade.

as $\nu_t/\nu = 0.09 Re_T$. A Reynolds number of 20.6 then gives $\nu_t/\nu = 1.85$. This means that the turbulence is rather weak, although its diffusive effects are still stronger than the viscous forces. On the other hand, the validity of the standard (that is, "high Re") k-ε at this value of the turbulence Reynolds number can be questioned. When introducing low-Reynolds number modifications, the expression becomes $\nu_t/\nu = C_\mu f_\mu Re_T$. From [29], $f_\mu = \exp(-3.4/(1 + Re_T/50)^2)$, which for $Re_T = 20.6$ gives $\nu_t/\nu = 0.34$. It should, however, be noted that this empirical function can be interpreted to primarily emulate near-wall effects rather than effects of weak turbulence.

3. Short cascade at low Reynolds numbers

The cascade model was developed under the assumption of a "high" Reynolds number. If the Reynolds number is reduced, the number of levels in the cascade will also be reduced. Approaching the limit, the shrinking cascade has only three or two levels, and finally just one.

The objective of this section was to investigate the potential effects of a small number of levels in the cascade, as a consequence of a low turbulence Reynolds number. When these effects are revealed, further work on modifying the cascade and related expressions can be pursued.

A three-level cascade is outlined in Fig. 1. For each level, the inertial energy transfers w_n and viscous dissipation q_n are denoted in the figure. Similar descriptions can be made for any number, N, of cascade levels. The general relation between the characteristic strain rates (frequencies), $\omega_n = \omega_{n-1}$, is fundamental for the cascade model and is maintained: $\omega^* = 2\omega''$ and $\omega'' = 2\omega'$; thus $\omega^* = 4\omega'$. Energy balances can be combined to express the fine-structure velocity and length scales as

$$u^* = \left(\frac{4^N}{4^N-1}\right)^{1/4} \cdot \left(\frac{C_{D2}}{3C_{D1}^2}\right)^{1/4} (\nu\varepsilon)^{1/4}. \tag{20}$$

and

$$L^* = \left(\frac{4^N-1}{4^N}\right)^{1/4} \cdot \frac{2}{3}\left(\frac{3C_{D2}^3}{C_{D1}^2}\right)^{1/4} \left(\frac{\nu^3}{\varepsilon}\right)^{1/4}. \tag{21}$$

The turbulence Reynolds number that give a cascade of N levels can be expressed as

$$(Re_T)_N = \left(4^0 + 4^1 + \cdots + 4^{N-1}\right)\frac{C_{D2}}{C_{D1}^2} = \frac{4^N-1}{4-1}\frac{C_{D2}}{C_{D1}^2} = (4^N-1)\frac{C_{D2}}{3C_{D1}^2}. \tag{22}$$

The parenthesis is a geometric series, which can be expressed as shown in the 2nd and 3rd equalities. The expressions can reformulated to

$$\left(\frac{4^N}{4^N-1}\right) = \left(1 + \frac{1}{Re_T}\frac{C_{D2}}{3C_{D1}^2}\right). \tag{23}$$

This can be introduced into Eqs. (20)–(21), leading to more general expression, developed for both high and low turbulence Reynolds numbers. Since the quantities of the cascade are based on averages (e.g. k and ε), the cascade itself represents an average, and the number of cascade levels needs not be an integer. With the relation $u'^2 = \frac{2}{3}k$, the fine-structure region mass fraction can be expressed as

$$\gamma_\lambda = \frac{u^*}{u'} = \left(1 + \frac{1}{Re_T}\frac{C_{D2}}{3C_{D1}^2}\right)^{1/4} \left(\frac{3C_{D2}}{4C_{D1}^2}\right)^{1/4} \left(\frac{\nu\varepsilon}{k^2}\right)^{1/4}, \tag{24}$$

while the fine-structure time scale becomes

$$\tau^* = (\dot{m}^*)^{-1} = \frac{L^*}{2u^*} = \left(1 + \frac{1}{Re_T}\frac{C_{D2}}{3C_{D1}^2}\right)^{-1/2} \left(\frac{C_{D2}}{3}\right)^{1/2} \left(\frac{\nu}{\varepsilon}\right)^{1/2}. \tag{25}$$

Consequently, the fraction γ_λ gets a slight increase at low Re_T. With this formulation, the value of $\gamma_\lambda = 1$ is reached at $Re_T = 27.4$, as compared to 20.6 for the original formulation. The two functions are compared in Fig. 2. The near-wall adaption of γ_λ by Myhrvold [23] (pp. 95–104) is shown, as well.

From the development above can be concluded that the few-level cascade 1) led to a larger value of γ_λ, that is, in the "wrong" direction if the aim was to lower γ_λ at low Re_T, 2) the changes were quite small, and 3) the need for a modification remained to avoid a non-physical value of the quantity. Accordingly, the still required modification would overrule the small differences between the original and the few-level expressions. Modifications can be based on the original expressions, rather than the present development for a short cascade.

4. EDC reaction rate model modified for low Reynolds and Damköhler numbers by Parente and co-workers

4.1. Background and described ideas

The modified EDC by Parente et al. [3,4] includes the turbulence Reynolds number, Re_T, and the small-scale Damköhler number, Da_η, in the expressions for γ_λ and τ^* (Eqs. (10)–(11)) and, thereby, in the mean reaction rate, Eq. (13). The variant by Lewandowski et al. [5,11] can be seen as a more stringent development of the same model, rather than a separate model. However, the model expressions have some differences and will be treated here as a separate variant. In the following it is denoted as "Lewandowski/Parente", while the former as "Parente/Evans".

An amendment of Parente's model was initially made by Bao [6] with a follow-up by Romero-Anton et al. [7]. They arrived a slightly different version of the modifications. Below, this is denoted as the "Bao/Romero" version. Recently, Fordoei et al. [8] presented another amendment.

The work of Parente and co-workers was partly motivated by the findings of De et al. [30] and others on the constants of EDC and the limit of validity for low Reynolds numbers. These findings were discussed in [2] and found to be based on the particular implementation of EDC in Fluent, and not a feature of EDC as such. Nevertheless, the modifications of Parente and co-workers can be plausible in their own right, irrespective of the incentives.

A first observation was that all said authors [3–7] maintained the relations following from the original cascade model [17], that is, the expressions of Eqs. (3)–(4) and the expression for the fine-structure Reynolds number, $Re^* = u^* L^*/\nu$. Although not explicitly stated, however implicit from Eqs. (3)–(4), they also maintained the expressions for L^* and u^*, Eqs. (5)–(6), and the viscous part of dissipation, Eqs. (8)–(9).

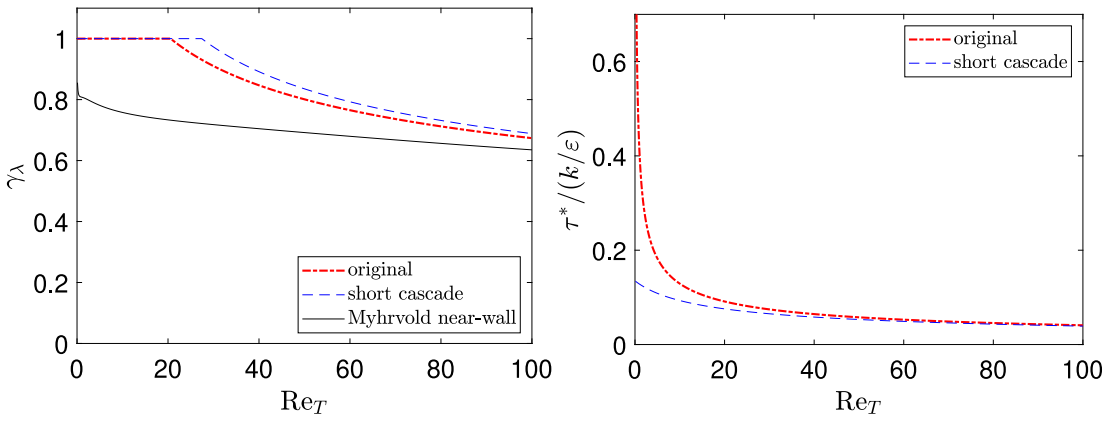

Fig. 2. γ_λ and τ^* for a short cascade, and Myhrvold's near-wall adaption [23] (pp. 95–104), compared to the original expression. Here, the limit $\gamma_\lambda < 1$ is applied.

Second, they maintained the expressions for the fine-structure region mass fraction γ_λ, Eq. (10), and the fine-structure exchange time scale τ^*, Eq. (11).

Third, all said authors determined a chemical time scale τ_c from a chemical mechanism, using local thermodynamic properties. Their practical choices were either based on a global, one-step reaction [3,7], or on the reaction rates of selected major species [4,5].

In the modifications to EDC, the concept of a turbulent flame speed S_T was introduced [3] with the relation

$$u^* \sim S_T \approx S_L \left(\frac{\nu_t}{\nu} + 1\right)^{1/2}, \tag{26}$$

where S_L is the laminar flame speed and $\nu_t/\nu \sim Re_T$. Both Parente/Evans and Bao/Romero set $\nu_t/\nu = Re_T$, while Lewandowski set $\nu_t/\nu = C_\mu Re_T$ with $C_\mu = 0.09$ (from most widely used k-ε and k-ω models).

A relation between chemical time scale, fine-structure length scale and laminar flame speed was formulated as

$$\tau_c = \frac{L^*}{S_L}. \tag{27}$$

It was noted that Bao/Romero distinguished between the fine-structure chemical timescale, τ_c^*, expressed from Eq. (27), and the chemical timescale, τ_c, determined from a chemical mechanism. However, they set the two equal, $\tau_c^* = \tau_c$. Parente/Evans and Lewandowski did not make this distinction.

Parente/Evans and Lewandowski/Parente made use of the relation $S_L = (\nu/\tau_c)^{1/2}$ for the laminar flame speed. Bao/Romero avoided use of that relation, and used $S_L = L^*/\tau_c$ (Eq. (27)) with the assumption $L^* = \eta$.

Some preliminary comments that can be made, are

– the assumption $L^* = \eta$ (by Bao/Romero) raises a question about inconsistency when already adopting Eqs. (3)–(4), which lead to Eqs. (5)–(6).

– the S_T to S_L relation shown in Eq. (26) is one of several different relations based on certain empirical data and limited to certain cases.

– the definition and understanding of S_T in a distributed reactions regime may not be obvious.

– On the other hand, when the turbulence Reynolds number becomes low, the fraction of the mass included in the fine structures (i.e. γ_λ^2) approaches unity, or exceeds unity if not bounded. That situation may require some consideration of the "internal" flame structure of the reactor of EDC.

4.2. Modified expressions, Parente/Evans

The fine-structure region mass fraction and time scale were expressed as Eqs. (10)–(11), however, with the constants C_γ and C_τ modified [3] to coefficients depending on the local Reynolds and Damköhler numbers,

$$C_\gamma = C_{\gamma 0}\left(Da_\eta(Re_T + 1)\right)^{1/2}, \tag{28}$$

$$C_\tau = C_{\tau 0} Da_\eta^{-1}\left(Re_T + 1\right)^{-1/2}, \tag{29}$$

with $Re_T = k^2/(\nu\varepsilon)$. Initially, the relations were proportional expressions [3], and constants were later set to $C_{\gamma 0} = \sqrt{2/3}$ and $C_{\tau 0} = 0.5$[4]. These functions were constrained [4] as $0.50 \le C_\gamma \le 2.14$ and $0.408 \le C_\tau \le 5.0$. It can be noted that the value $C_{\gamma 0} = \sqrt{2/3}$ implied that a tuning factor of 2/3 was multiplied into the expression, as the development gave the value $\sqrt{3/2}$ (cf. [5,11]).

The upper limit of C_γ and the lower limit of C_τ were set to the standard values of these constants. For each value of Da_η, these limits provide upper Re_T limits for the effects of the modifications.

The modifications were motivated by an observed over-prediction of the mean reaction rate, leading to overestimate of temperatures in MILD combustion. An aim was to limit the reaction zone and to achieve a longer reaction residence time [4]. Evans et al. [4] tried the formulation for two of the Adelaide jet-in-hot-coflow flames.

Some of the relevant EDC quantities are shown in Fig. 3 as functions of the turbulence Reynolds number Re_T and some values of the Damköhler number Da_η. The fine-structure region mass fraction γ_λ was expressed from Eq. (10) with Eq. (28), while the timescale ratio $\tau^*/(k/\varepsilon)$ from Eq. (19) using Eq. (29). For higher Da_η, the modifications had lesser effects and the quantities came closer to the standard model. It should be noted that in Fig. 3 and subsequent graphs, γ_λ is presented with the limitation $\gamma_\lambda < 1$ for all models, whereas in practice, a lower limit might be used to avoid a singularity in Eq. (13).

It was seen that for $Da_\eta = 0.05$, C_γ is modified for $Re_T < 136$, while for lower Re_T at higher Da_η, the $\gamma_\lambda < 1$ constraint will be needed. At $Da_\eta > 0.33$, the expression gives $\gamma_\lambda > 1$ for a range of Re_T below 20.

For the sake of comparison, Fig. 3f was made with a deviation from the standard EDC by using $n = 3$ (not $n = 2$) in the denominator of Eq. (13), and by setting $\chi = 1$.

The effect of the C_τ modification is seen over a wider range of the Reynolds number. For $Da_\eta = 0.1$, C_τ is modified for $Re_T < 149$; for $Da_\eta = 0.2$, C_τ is modified for $Re_T < 36$; for $Da_\eta = 1$, C_τ is modified only for $Re_T < 0.5$.

Worth noting is that, for low Da_η, the ratio of the fine-structure time scale τ^* to the turbulence turn-over time scale k/ε can exceed unity for low Re_T. The physicality of this can be questioned. For instance, Durbin [31] introduced the Kolmogorov time scale as a lower limit for the turbulence transport (or mixing) time scale, k/ε. For the standard model, this limit is achieved for $Re_T > C_\tau^2 = 0.17$, cf. Eq. (19). With Eq. (29), the limitation is reached at Re_T of 4.5 and 9.5, respectively, for Da_η of 0.1 and 0.05.

The lower limit of C_γ has an impact only for $Da_\eta < 0.17$, while the upper limit of C_τ affects the value for $Da_\eta < 0.1$.

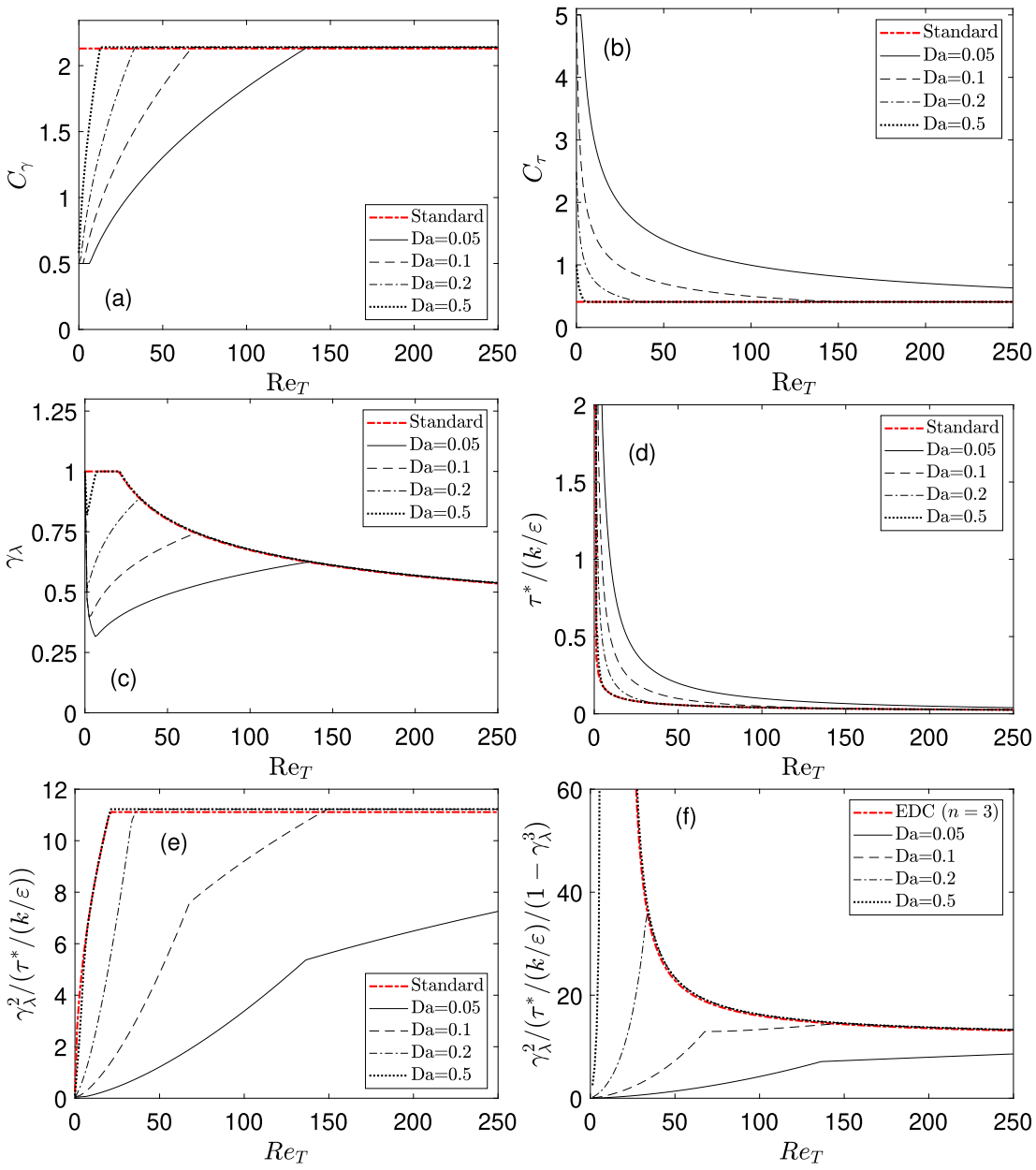

Fig. 3. EDC quantities as functions of the turbulence Reynolds number Re_T, standard EDC (notice $n = 3$ and $\chi = 1$ (cf. Eq. (13)) in (f)) and Parente/Evans modifications, Eqs. (28)–(29), for specified Da_η values (with $\gamma_\lambda < 1$).

4.3. Lewandowski/Parente modifications

Lewandowski et al. [5,11] used the relations from Parente/Evans (see above), except that the constant $C_\mu = 0.09$ was retained in the expression for ν_t/ν (cf. Eq. (26)):

$$C_\gamma = C_{\gamma 0}\left(Da_\eta(0.09Re_T + 1)\right)^{1/2}, \tag{30}$$

$$C_\tau = C_{\tau 0}Da_\eta^{-1}\left(0.09Re_T + 1\right)^{-1/2}. \tag{31}$$

Furthermore, $C_{\gamma 0} = \sqrt{3/2}$ was obtained from the development [3] and not multiplied with any tuning coefficient. $C_{\tau 0} = 0.5$ and the constraints $0.50 \le C_\gamma \le 2.14$ and $0.408 \le C_\tau \le 5.0$ were maintained from [4]. Deviating from Parente/Evans (and Bao/Romero), Lewandowski/Parente used Eq. (13) with $n = 2$ and $\chi \le 1$ from Eqs. (14)–(18). They tried the formulation for five cases of the Delft jet-in-hot coflow flames and six cases of the Adelaide jet-in-hot coflow flames.

Results for the version of Lewandowski et al. [5] are shown in Fig. 4 and compared to standard EDC. Note that for the comparison, Fig. 4f was made with $\chi = 1$ for both models, to avoid selecting another range of parameters for χ. The effects are similar to those of the Parente/Evans version, Fig. 3, however, stronger and acting over a wider range of turbulence Reynolds number. Both versions reduce C_γ and γ_λ and increase C_τ and τ^* in a range of relatively low values of Re_T. Both these effects contribute to a reduced mean reaction rate, as shown in Figs. 3f and 4f.

It is worth noting that in Lewandowski's "hybrid" model [5,11], C_γ and C_τ of Eqs. (30)–(31) switched to the standard values of the constants for $Re_T < 28$ for any value of Da_η. This switch is not reflected in Fig. 4.

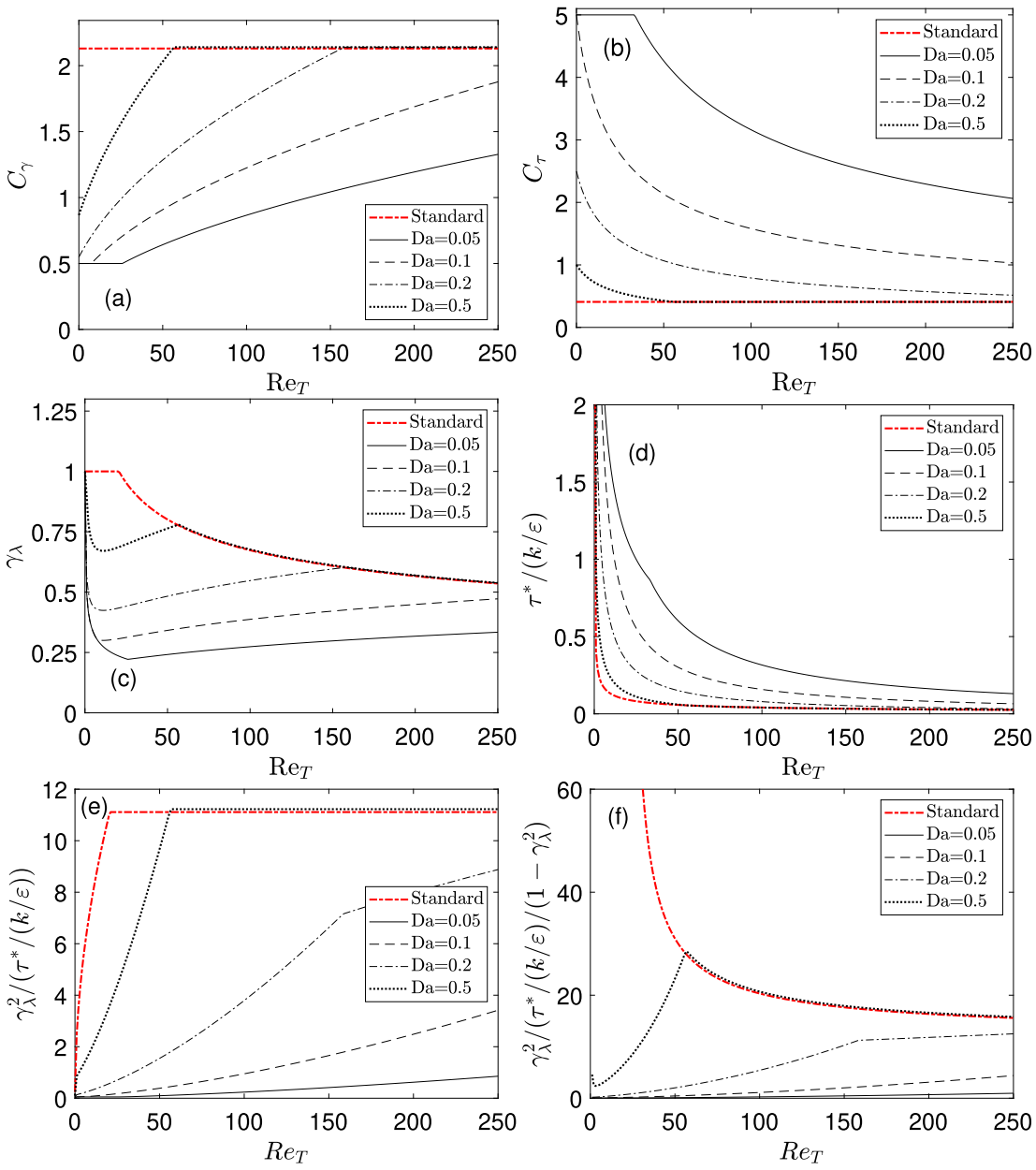

Fig. 4. Lewandowski version — EDC quantities as functions of the turbulence Reynolds number Re_T, standard EDC and modifications of Eqs. (30)–(31) for specified Da_η values ($\chi = 1$ for all in (f)). Limit $\gamma_\lambda < 1$ for all.

4.4. Modifications by Bao/Romero

In the work of Bao [6] and Romero-Anton et al. [7], C_γ was expressed as

$$C_\gamma = C_{\gamma 0} Da_\eta^{3/4} \left(Re_T + 1\right)^{1/2}, \tag{32}$$

with $C_{\gamma 0} = \sqrt{2/3}$, while Eq. (29) for C_τ was maintained. The coefficients were constrained as $2.1377 \le C_\gamma \le 13$ and $0.2 \le C_\tau \le 0.4083$, and the limitation $\gamma_\lambda < 1$ was imposed. (N. Romero-Anton, personal communication, Nov.-Dec. 2020.)

Comparing the expressions, Eq. (32) can be seen as Eq. (28) multiplied with $Da_\eta^{1/4}$ on the right-hand side. Furthermore, Parente/Evans constrained the coefficients such that C_γ was less or equal, and C_τ greater or equal, to the standard values. Bao/Romero did it the other way, such that C_γ was greater than or equal, and C_τ less or equal, to the standard values.

Also these authors mentioned reduced temperature and longer chemical time scales in MILD combustion compared to conventional combustion as a motivation. They tried the formulation against experimental data for the Delft lab-scale furnace for flameless (aka. MILD) combustion [32]. The ranges of Re_T and Da_η for this case was not found. However, compared to the Adelaide flames, the flame is wider and with lower flow velocity. The former may tend to increase the turbulence Reynolds number, while the latter clearly reduces it. A rough estimate may place the furnace flame in-between the cases of the Adelaide flames in the regime diagram (Da_η-Re_T diagram or a Borghi diagram).

Resulting quantities for the Bao/Romero version are shown in Fig. 5. The notable differences from the Parente/Evans version were that C_γ and γ_λ increased, while C_τ and τ^* decreased, rather than opposite. This contributed to an increase in the mean reaction rate, as seen in Fig. 5f. Due to the increase of γ_λ, this quantity had to be limited to avoid increase above unity.

The effects occurred at higher values of Re_T. In particular for low Da_η, the Bao/Romero modifications turned out identical to the standard EDC at low and moderate values of Re_T. The difference

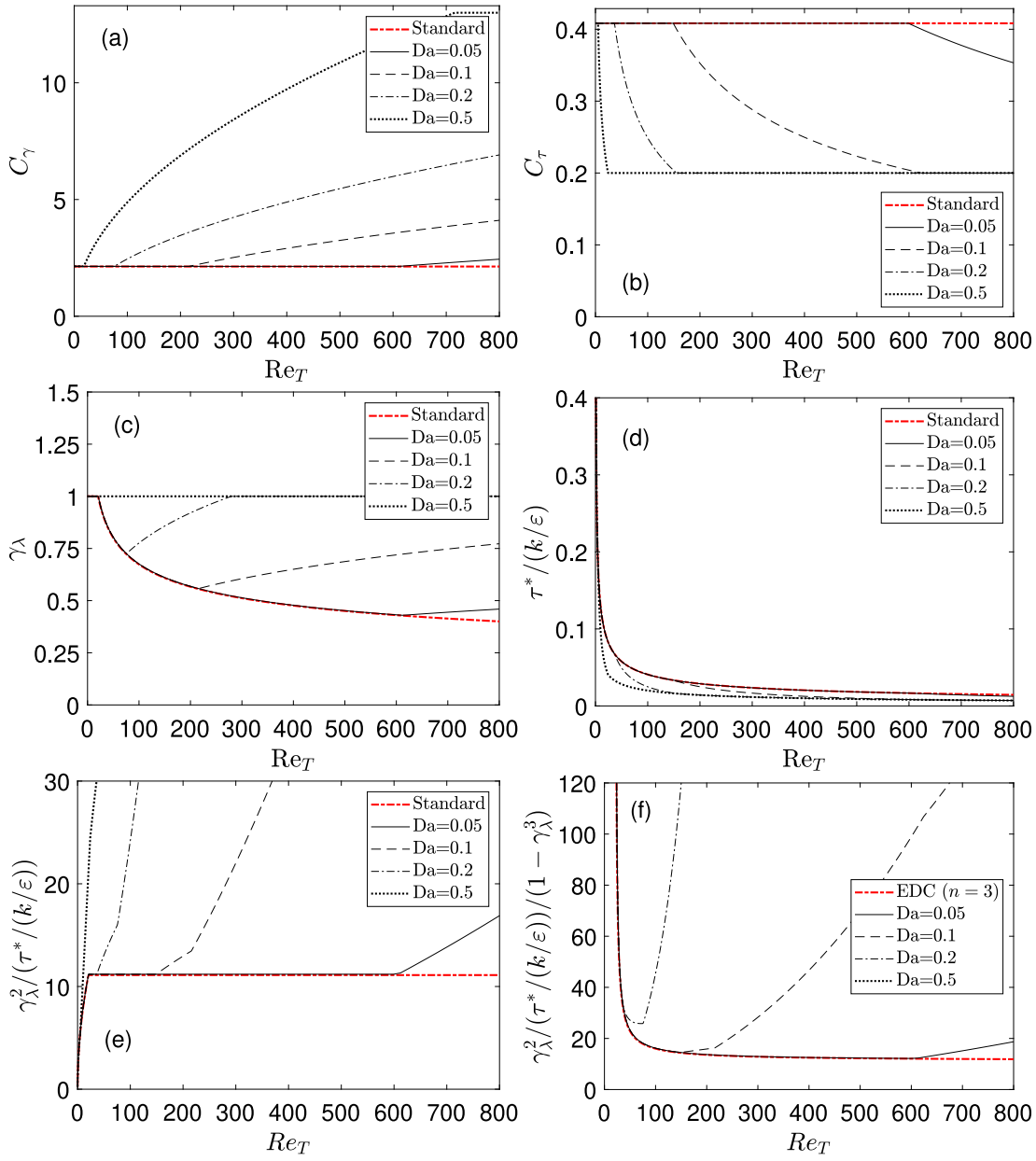

Fig. 5. EDC quantities as functions of the turbulence Reynolds number Re_T, standard EDC (note $n = 3$ and $\chi = 1$ (cf. Eq. (13)) in (f)) and modifications by Bao/Romero, Eqs. (29) and (32), for specified Da_η values. Limit $\gamma_\lambda < 1$ for all.

between the model expressions was the factor $Da_\eta^{1/4}$ multiplied into the expression for C_γ, as mentioned above. This factor damped the effect on increasing C_γ and γ_λ.

4.5. Modifications by Fordoei et al.

In a recent paper, Fordoei et al. [8] used the expressions of Parente, Eqs. (28)–(29), in combination with the χ expressions of Magnussen and Gran [18,20,22]. The constants were set to $C_{\gamma 0} = 0.5$ and $C_{\tau 0} = 0.0774$. The paper suffered from a few typographical errors, but the coefficients appeared to be constrained as $2.1377 \le C_\gamma \le 5$ and $0 \le C_\tau \le 0.4082$. Furthermore, the turbulence Reynolds number was printed as the square root of the expression used above. However, as a direct reference to [3], it was regarded as a typo, and the usual definition was maintained here. Constraining γ_λ to be less than unity was not mentioned, however assumed here for reasons mentioned in Section 4.2.

The values of $C_{\gamma 0}$ and $C_{\tau 0}$ were referred to [3]. Although not specified in the cited paper, also [11] referred to this source for the same values.

For motivation, this paper referred to Parente et al. [3] and aimed to reduce the mean reaction rates. Fordoei et al. [8] tried the formulation against experimental data for MILD combustion of a jet in hot coflow in the Lisbon furnace [33,34]. This flame had an air coflow jet Reynolds number of 14000, which placed it in-between the Adelaide cases in the regime (Da_η-Re_T) diagram. That is, in a moderate or relatively low turbulence Reynolds number range. It was noted that Fordoei et al. used the χ of Eqs. (14)–(16).

Results are shown in Fig. 6, where some similarities with the Bao/Romero version are observed.

4.6. Effects of limits imposed on locally determined coefficients

All variants of the modified EDC came with limits on C_γ and C_τ. It was observed that for the Parente/Evans and Lewandowski/Parente

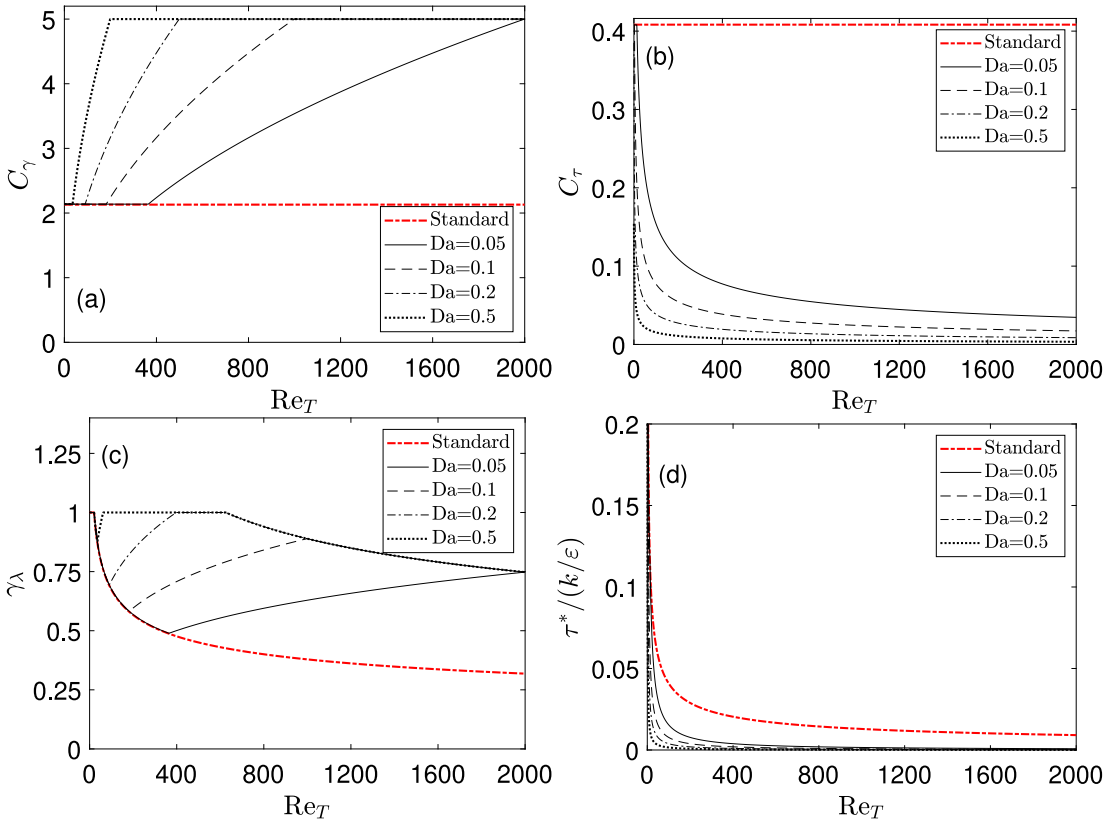

Fig. 6. EDC quantities as functions of the turbulence Reynolds number Re_T, standard EDC and modifications by Fordoei et al. [8], for specified Da_η values. Limit $\gamma_\lambda < 1$ for all.

versions, standard EDC constants were set as the limit at high Damköhler numbers and high Reynolds number. For low values of Re_T and Da_η, C_γ was set to a lower value, while C_τ was set to a value higher than the standard EDC constants.

For the Bao/Romero and Fordoei versions, the chosen limits were the opposite: The standard values were the limit at low values of Re_T and Da_η. For high Re_T and high Da_η, C_γ was set to a high value, while C_τ was set to a value lower than the standard EDC constants. For the Fordoei version, no lower constraint was specified for C_τ.

The importance of the constraints on C_γ and C_τ can be seen by comparing Fig. 3a to Fig. 5a for C_γ and Fig. 3b to Fig. 6b for C_τ. An unrestricted raise of C_γ can readily be imagined from the graphs. It was noted that C_γ from Eqs. (28), (30) and (32) will give an unlimited increase in C_γ and γ_λ with increasing Re_T, unless restricted. The upper constraint on C_γ prevents this increase for high Re_T. For low Re_T, a range of Da_η can still give $\gamma_\lambda > 1$, and the expressions have to be supplemented by another constraint. Some quantities resulting from the low and high Re_T and Da_η limits of Parente/Evans (Lewandowski/Parente coincides) and Bao/Romero are shown in Table 2.

Fig. 7 shows the effects on the fine-structure length scale L^* for the different versions, as resulting from the cascade model. The small values obtained by the Fordoei version, Fig. 7d, are primarily caused by the lack of a lower limit to C_τ. It should be noted that Bao/Romero, besides maintaining the cascade model, Eqs. (3)–(4), leading to Eq. (5), also used the Kolmogorov length for L^* in some of the expressions derived from Parente et al. This dual usage of L^* appears as an inconsistency. The results of L^*/η in this subsection were based on the cascade model. The version reached the high limit of L^*/η at relatively high values of Re_T (Fig. 7c).

In order to visualize the differences between Parente/Evans and Bao/Romero, the latter version was run with the constraints of the former. That is, Eq. (32) for C_γ and Eq. (29) for C_τ with the constraints $0.50 \le C_\gamma \le 2.14$ and $0.408 \le C_\tau \le 5.0$ (from [4]). Results are shown in Fig. 8. Comparison with Figs. 3 and 7a shows the effect of the different exponents of Da_η in Eqs. (32) and (28) for C_γ. For C_τ and τ^*, the results were identical to Parente/Evans. Comparing Fig. 8 with Figs. 5 and 7c shows the effects of chosen constraints to C_γ and C_τ.

4.7. Exploring the modifications

The constraints on C_γ, C_τ and γ_λ will limit the ranges of Da_η and Re_T values where the modifications have effect, as pointed out by Lewandowski [5,11]. This is shown in Fig. 9 (cf. Fig7.2 of [11]). For instances where a Da_η, Re_T combination is above the upper limits (lines for $C_{\gamma,\max}$ and $C_{\tau,\min}$), the standard constants will be used. It is seen that the Lewandowski/Parente version influences wider ranges of Da_η and Re_T values than the Parente/Evans version.

The constraint $\gamma_\lambda < 1$ will still be active, but does not influence the use of the modifications unless at low Re_T values. Below the lower limits, lines for $C_{\gamma,\min}$ and $C_{\tau,\max}$, the modifications will simply be to use the original expressions with adjusted constants.

Parente/Evans set $C_{\gamma,\max}$ and $C_{\tau,\min}$ to the standard constants, while Bao/Romero set $C_{\gamma,\min}$ and $C_{\tau,\max}$ to these values. Accordingly, the latter version returns to the standard version *below* the lower lines in Fig. 10, that is, at low Re_T and low Da_η. Above the $C_{\tau,\max}$ line, the original τ^* formulation is used, with a modified constant. With the $\gamma_\lambda < 1$ limitation, C_γ does not reach the upper limit unless at very high Re_T ($2.9 \cdot 10^4$) at above $Da_\eta = 0.043$.

In summary, different versions of the modifications show effects at different ranges of Da_η and Re_T. Effects are seen at higher Da_η and Re_T values for Bao/Romero than for Parente/Evans.

The ratio of the viscous term to the total dissipation, as described by Eq. (9) above, can be evaluated for the variants of the modified EDC. The resulting profiles are shown in Figs. 11 and 12. The major difference seen was that while Parente/Evans and Lewandowski/Parente damped the viscous contribution at lower values of Re_T and Da_η, the

Table 2
EDC quantities resulting from the limiting values at low and high values of Re_T and Da_η for Parente/Evans (also Lewandowski/Parente) and Bao/Romero; reaction-rate constant (Eq. (12)), fine-structure scales (Eqs. (5)–(7)), viscous term of dissipation (ϵ_2/ϵ, Eq. (9)).

Re_T and Da_η	C_γ	C_τ	C_{D1}	C_{D2}	C_R	L^*/η	v^*/v_K	Re^*	Re_T at $\epsilon_2/\epsilon = 0.10$
P/E low limit	0.5	5.0	30	75	0.05	4.08	4.08	1.67	0.68
P/E high limit	Coincides with standard EDC								
B/R low limit	Coincides with standard EDC								
B/R high limit	13	0.2	0.0018	0.12	845	4.25	10.6	45.1	$3.1 \cdot 10^5$
Standard	2.130	0.4082	0.135	0.50	11.1	1.42	1.74	2.47	222

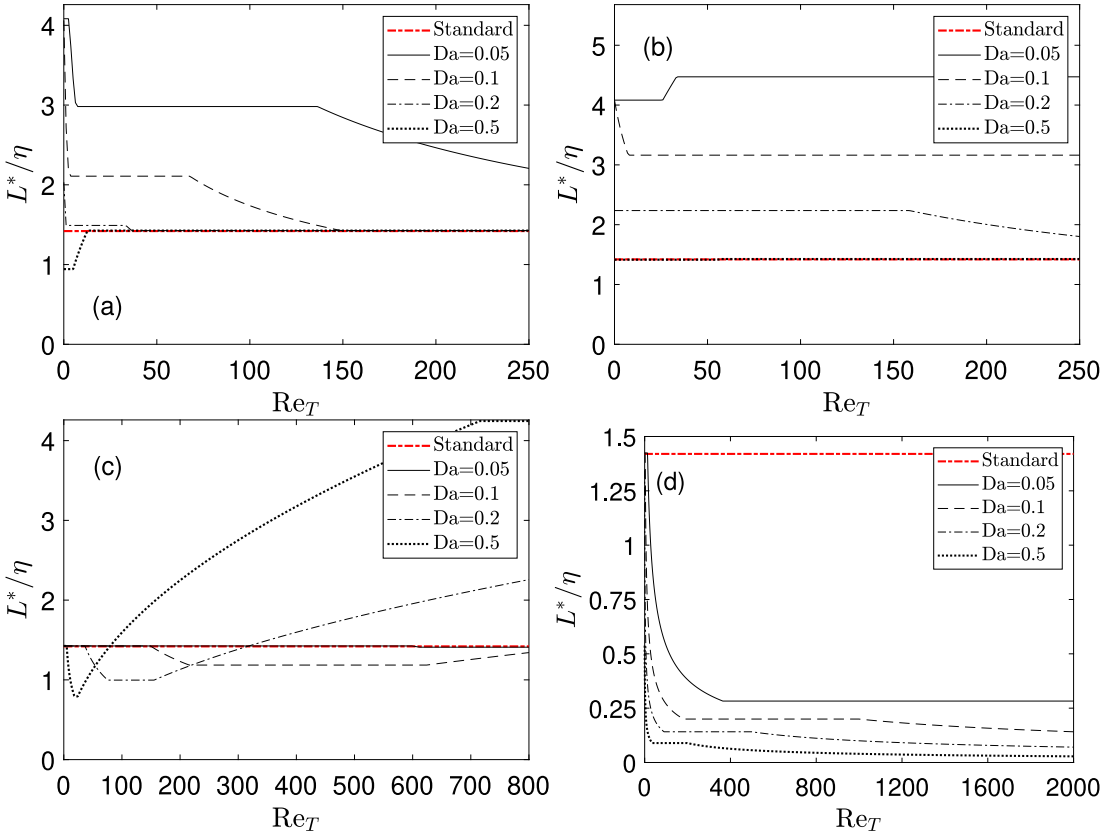

Fig. 7. Fine-structure length scale from (a) Parente/Evans, (b) Lewandowski/Parente, (c) Bao/Romero (note remarks in the text) and (d) Fordoei modifications as functions of the turbulence Reynolds number Re_T for specified Da_η values.

version of Bao/Romero increased the viscous contribution at higher values of these parameters. Following this, in the non-reacting limit, the former two versions gave a very low viscous contribution (based on minimum C_γ), while the latter returned to the original values in this limit (standard C_γ as the minimum). For a high Da_η, the Bao/Romero version led to a very high contribution of the viscous term, based on the maximum C_γ. In Fig. 12, this is seen for $Da_\eta = 0.5$ for $Re_T > 800$.

4.8. A comparison with the standard EDC

The modifications reviewed above [3,4,7] were based on the EDC reaction rate, Eq. (13), formulated with $n = 3$ and $\chi = 1$, while [5] had $n = 2$ and [8] had $n = 3$, both with $\chi \leq 1$ from [20,22] (Eqs. (14)–(18) above).

The analysis of Lewandowski and Ertesvåg [22] showed that inclusion of the non-unity χ of Eqs. (14)–(16) made significant improvement to the results for the Delft jet-in-hot-coflow case. Therefore, it was interesting to compare the modified models with the original, employing a non-unity χ.

A comparison is shown in Fig. 13, including Parente/Evans and Lewandowski/Parente. For all models a "practical" limit of $\gamma_\lambda \leq 0.8$ was chosen. Effects of clipping of γ_λ to values below unity was discussed by Lewandowski and Ertesvåg [22]. For the two modified models, $Da_\eta = 0.20$ was chosen, since this is a value where both γ_λ and τ^* are modified in both extended variants, cf. Fig. 9. For the standard EDC, the quantities are shown for $\chi = 1$, and for χ evaluated at two different values of the reaction progress variable c, Eqs. (14)–(18), the Lewandowski/Parente model for one value of c, and both models for local stoichiometric mean mixture. The fine-structure mass fraction γ_λ^n (see Eq. (13)) was evaluated with $n = 3$ for the Parente/Evans model (Figs. 13c and 13d), while both with $n = 3$ (Fig. 13c) and with the recommended $n = 2$ (Fig. 13d) for the standard EDC. Lewandowski/Parente had $n = 2$ (Fig. 13c).

The results showed that the standard EDC can match well inside the range of the results of the modified models. A possible explanation is that the reaction progress variable, based on the local mean composition, actually reflects effects of the chemical time scales, similar to the Damköhler number.

One effect of including χ_2 is a reduction in the mean reaction rate for incompleted reactions (overall $c < 1$). This matches the effect of a low Damköler number. Slow chemical reactions lead to uncompleted reactions within the reactor. Another effect of χ_2 is a reduction in the mean reaction rate for low turbulence Reynolds numbers. Both these effects contributes to explaining the results seen in [22].

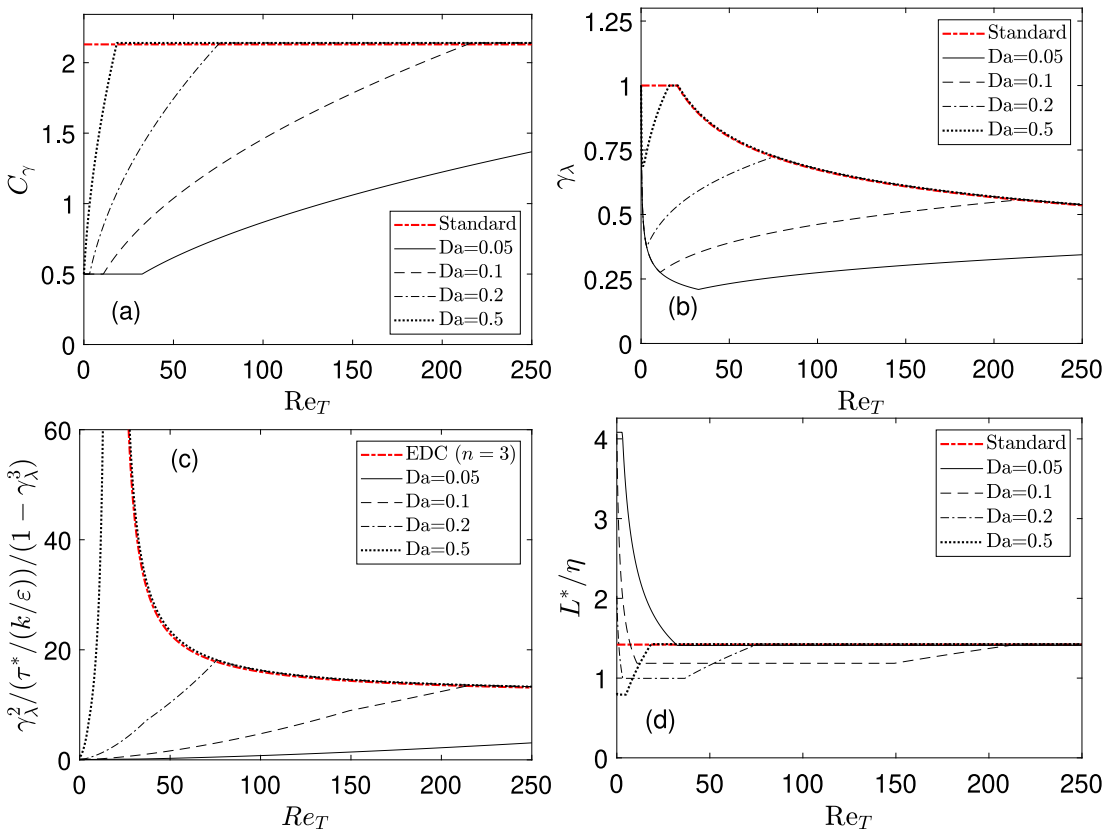

Fig. 8. EDC quantities as functions of the turbulence Reynolds number Re_T for specified Da_η values; Bao/Romero modifications, Eqs. (32) and (29), with constraints from Parente/Evans. Limit $\gamma_\lambda < 1$ in (b) and (c); standard EDC deviated with $n = 3$ and $\chi = 1$ in (c).

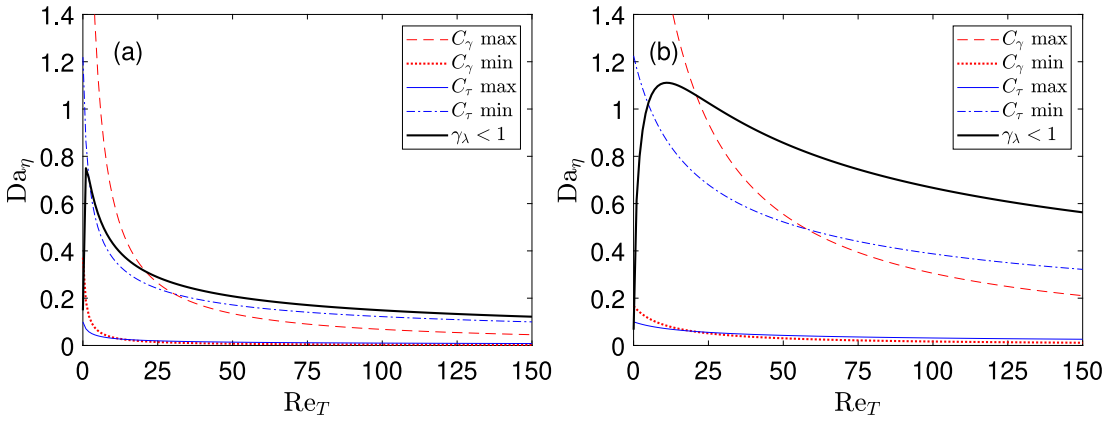

Fig. 9. Limits of Da_η where modifications take effects: Lower limits made by $C_{\gamma,\min}$ (=0.50) and $C_{\tau,\max}$ (=5.0). Upper limits made by $C_{\gamma,\max}$ (=2.14), $C_{\tau,\min}$ (=0.408) and $\gamma_\lambda < 1$. (a) Parente/Evans and (b) Lewandowski/Parente.

5. Discussion

A basic criticism of the EDC has been that the cascade model was developed for high turbulence Reynolds numbers, Re_T, and that its effects and validity in weak turbulence are uncertain. The extended EDC formulations did not address this issue. All versions discussed here accepted the cascade in its original formulation. Above, the cascade expressions were formulated to be used over any number of steps. Although without solving the issues, doing this minor task was necessary to remove the uncertainty, before dealing with the challenges of modifying the model.

In weak turbulence, that is, low Re_T, the need to avoid γ_λ reaching unity has been obvious in the original EDC. None of the investigated modifications or extensions remove this need. On the contrary, some versions require imposing a less-than-unity limit on γ_λ at a wider range of Re_T. Consequently, when such a limitation has to be used, the choice of limiting value determines the reaction rate. For instance, the Delft Jet-in-hot-coflow flame had a range of Re_T below 100, for a large part below 40, see [5] (their Fig. 2a). In this range, the choice of limiting value for γ_λ will be decisive for the reaction rate when the $\chi = 1$ assumption is made. The issue of limiting γ_λ at low Re_T still remains. An open question is whether it simply can be limited to some maximum value in the range, say 0.7-0.95, or if a more complex relation is required.

There is also an issue regarding the fine-structure time scale versus the turnover turbulence time. It is to a large extent related to the

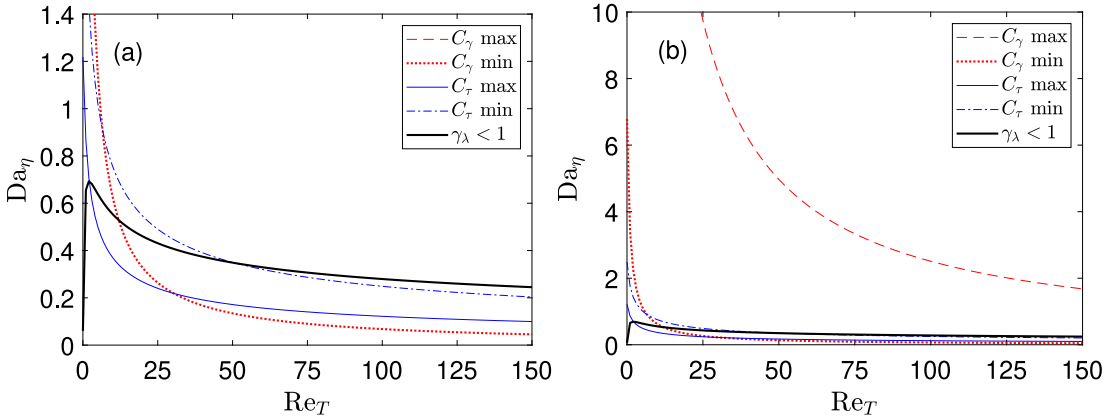

Fig. 10. Limits of Da_η where modifications take effect in the Bao/Romero version: Lower limits made by $C_{\gamma,\min}$ (=2.1377) and $C_{\tau,\max}$ (=0.4083). Upper limits made by $C_{\gamma,\max}$ (=13), $C_{\tau,\min}$ (=0.2) and $\gamma_\lambda < 1$. Upper limits made by $\gamma_\lambda < 1$. (a) axes similar to Fig. 9; (b) extended vertical axis.

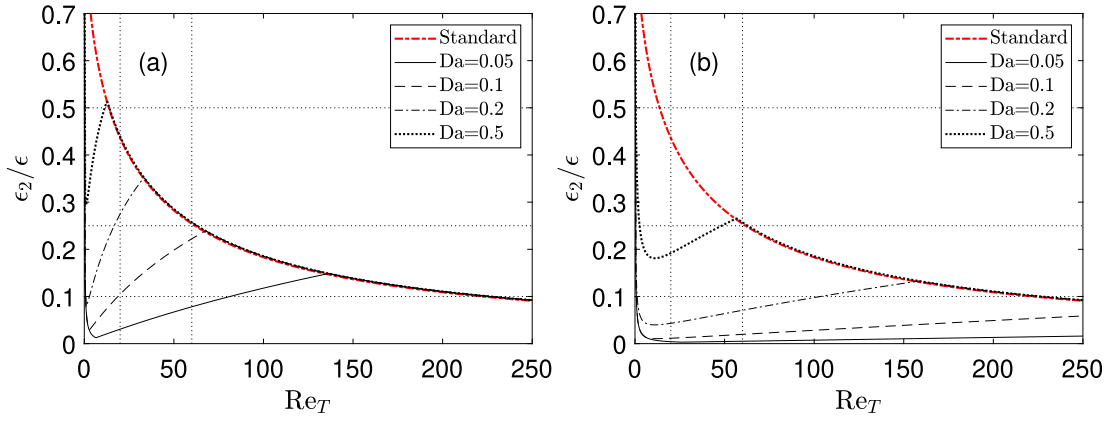

Fig. 11. Ratio of viscous term to the total dissipation rate, Eq. (9): (a) Parente/Evans and (b) Lewandowski/Parente versions for specified Da_η values compared with Standard EDC.

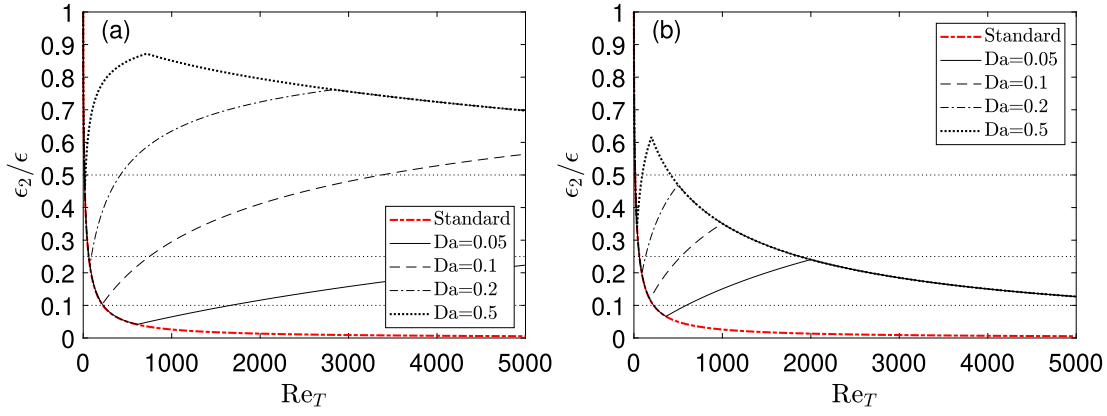

Fig. 12. Ratio of viscous term to the total dissipation rate, Eq. (9): (a) Bao/Romero and (b) Fordoei et al. versions for specified Da_η values compared with Standard EDC.

turbulence model, as it can be argued that the turbulence model should not let the Kolmogorov time scale exceed the turnover time. For the standard EDC, the ratio $\tau^*/(k/\varepsilon)$ can exceed unity only at very low Re_T (< 0.2). The modifications of Parente and co-workers [3–5] lead to reaching the limit at higher Re_T than the standard EDC. The locally determined C_τ can exceed unity, meaning that τ^* can exceed the turnover timescale (k/ε), even when the turbulence model prevents the Kolmogorov scale to do so.

When considering chemical time scale or Damköhler number effects on the mean reaction rate, it should be kept in mind that this is already inherent in EDC with finite-rate chemistry. The fine-structure reaction rate [2,20] is iteratively found as

$$R_k^*/\rho^* = (Y_k^* - Y_k^o)/\tau^*, \tag{33}$$

where ρ^* and Y_k^* are the reactor density and species mass fraction, and Y_k^o is the species mass fraction of the reactor inlet (well stirred reactor) or initial to the integration (batch reactor). The reaction rate is expressed from the kinetic model, usually an Arrhenius model. The left-hand side of Eq. (33) is the reciprocal of the chemical time scale for species k. By multiplying both sides by τ^*, or τ^*/C_τ, a Damköhler

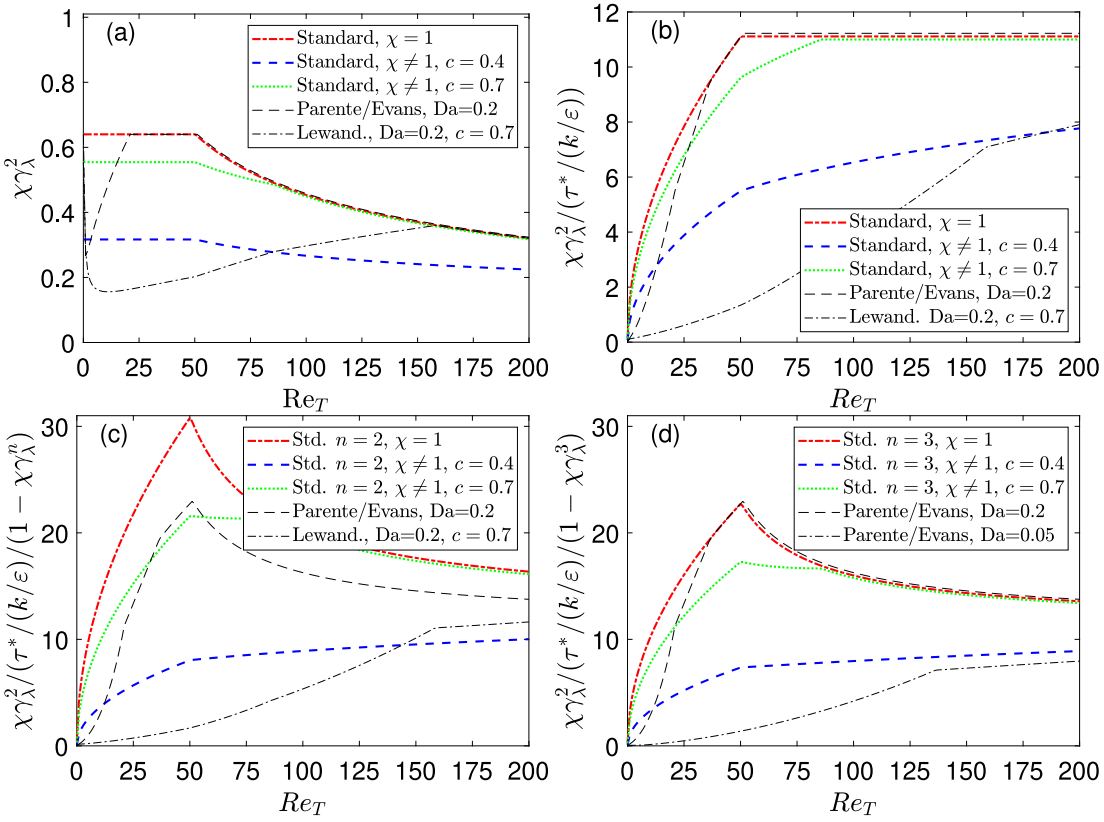

Fig. 13. EDC quantities as functions of the turbulence Reynolds number Re_T, standard EDC (with $n = 2$ in (c) and $n = 3$ in (d), Eq. (13)) and modifications by Parente/Evans ($n = 3$, $\chi = 1$) and Lewandowski ($n = 2$ and $\chi \neq 1$). $\gamma_\lambda \leq 0.8$ for all.

number appears. This consideration can also be made for the individual reactions, providing timescales for all elementary reactions.

The reaction rate or chemical time scale can limit the progress of the reaction, as can also the mixing conditions. Hence, the extent of reaction or progress variable c included in the fine-structure reacting mass fraction, χ, Eqs. (15)–(16), is closely related to the Damköhler number. This can explain why inclusion of χ led to the improved results [22] for the Delft jet-in-hot-coflow flame without any ad-hoc adaption of the standard EDC. For slow reactions (long chemical time, low Damköhler number), the reaction progress is delayed by the fine-structure reactor. Including the reaction progress in χ and the reaction rate, enhances this effect.

At this point it can be worth noting that practicalities and choices made in the implementation of any model into a code may not be reported in the publications. Such details can still influence on the flame results. This is not covered by the present study. Furthermore, features of a specific case can imply that the aspects and differences discussed here are less important for the overall results of the flame simulations.

Further work on developing EDC will have to consider the treatment for the low Re_T range, where the cascade collapses and the reactor mass approaches the total mass. This will lead to a reformulation of the length and velocity scales, u^* and L^*, at low Re_T and hence, of the fine-structure reactor mass fraction and timescale. Indeed, the concept of fine structures may need a revision under these conditions, when the fine-structure mass approaches the total mass. Subsequently, extended effects of the chemical timescale can be considered for this range. In this setting, the ideas outlined by Parente and co-workers might become fruitful. A possibility for future work will be to include more of the desired features in the quantity χ.

6. Concluding remarks

Modifications of EDC suggested by Parente and co-workers [3–5], including functions of the local turbulence Reynolds number Re_T and fine-scale Damköhler number Da_η, have been investigated and compared with the original standard EDC. Also the recent versions of Bao [6] and Romero-Anton et al. [7] and of Fordoei et al. [8] are examined.

Initially, the EDC cascade model formulations, originally based on high Reynolds numbers, have been rewritten to include also low Reynolds numbers with a short cascade. This expression gives results similar to the original model, and issues of very low turbulence Reynolds numbers still remain.

The variants of the modified or extended model give different effects. The Parente/Evans and Lewandowski/Parente modifications reduce the fine-structure region mass fraction γ_λ and increase the fine-structure time scale τ^* at low turbulence Reynolds numbers, while returning to standard EDC at higher Reynolds numbers. This explicitly stated aim of the modified model is clearly achieved. On the contrary, the modifications of Bao/Romero and Fordoei et al. maintain the standard EDC at low Reynolds numbers, while increasing γ_λ and reducing τ^* for higher turbulence Reynolds numbers. In particular, the Fordoei modifications give a very low τ^*.

Constraints, or lack of such, to the values of the locally determined C_λ and C_τ are decisive for the EDC quantities resulting from the extended model proposals. Differences in the constraints are more important than the variations in formulation. Moreover, the specific choice of limit for γ_λ will also be decisive for cases of low turbulence Reynolds numbers. A notable example is the Delft jet-in-hot-coflow flame, which falls in the range where a limit is required.

In general, the proposed modifications do not remedy the need to limit γ_λ at low turbulence Reynolds numbers. Moreover, for the versions

of Bao/Romero and Fordoei et al. a less-than-unity limit has to be imposed on γ_λ to avoid a negative mean reaction rate over a wide range of Re_T values at low Da_η.

The proposed modifications do not modify the cascade formulation, leaving its low-Reynolds-number challenges unresolved. All versions of the modifications lead to increasing viscous effects with increasing turbulence Reynolds number for a range of this number. In particular, the Bao/Romero and Fordoei versions lead to very strong viscous effects at a very high (10^3) turbulence Reynolds number.

Some of the effects intended by the modifications are already available in the standard EDC through the factor χ, which is left out in the models by Parente/Evans and Bao/Romero, while included by Lewandowski and by Fordoei et al.

CRediT authorship contribution statement

Ivar S. Ertesvåg: Conceptualization, Methodology, Software, Investigation, Data curation, Writing – original draft, Writing – review & editing, Visualization.

Declaration of competing interest

The authors declare that they have no known competing financial interests or personal relationships that could have appeared to influence the work reported in this paper.

Acknowledgments

The author appreciates discussions with phd student Bima A. Putra and postdoc Michał T. Lewandowski at NTNU.

This work was partially conducted as a contribution to the Fire Research and Innovation Centre (www.fric.no) initiated by the Research Council of Norway, Project No. 294649.

References

[1] Magnussen BF. On the structure of turbulence and a generalized Eddy Dissipation Concept for chemical reaction in turbulent flow. In: 19th. AIAA aerospace science meeting, Jan. 12-15, 1981. St.Louis, Missouri; 1981.

[2] Ertesvåg IS. Analysis of some recently proposed modifications to the Eddy Dissipation Concept (EDC). Combust Sci Technol 2020;192:1108–36. http://dx.doi.org/10.1080/00102202.2019.1611565.

[3] Parente A, Malik MR, Contino F, Cuoci A, Dally BB. Extension of the Eddy Dissipation Concept for turbulence/chemistry interactions to MILD combustion. Fuel 2016;191:98–111. http://dx.doi.org/10.1016/j.fuel.2015.09.020.

[4] Evans MJ, Petre C, Medwell PR, Parente A. Generalisation of the eddy-dissipation concept for jet flames with low turbulence and low Damköhler number. Proc Combust Inst 2019;37(4):4497–505. http://dx.doi.org/10.1016/j.proci.2018.06.017.

[5] Lewandowski MT, Parente A, Pozorski J. Generalised Eddy Dissipation Concept for MILD combustion regime at low local Reynolds and Damköhler numbers. Part 1: Model framework development. Fuel 2020;278. http://dx.doi.org/10.1016/j.fuel.2020.117743.

[6] Bao H. Development and validation of a new Eddy Dissipation Concept (EDC) model for MILD combustion. (Master's thesis), Netherlands: Delft University of Technology; 2017, URL resolver.tudelft.nl/uuid:45fdb951-408f-404f-8b9a-71f2eda6540b (Last accessed 29 Oct 2020).

[7] Romero-Anton N, Huang X, Bao H, Martin-Eskudero K, Salazar-Herran E, Roekaerts D. New extended eddy dissipation concept model for flameless combustion in furnaces. Combust Flame 2020;220:49–62. http://dx.doi.org/10.1016/j.combustflame.2020.06.025.

[8] Fordoei EE, Mazaheri K, Mohammadpour A. Numerical study on the heat transfer characteristics, flame structure, and pollutants emission in the MILD methane-air, oxygen-enriched and oxy-methane combustion. Energy 2021;218:119524. http://dx.doi.org/10.1016/j.energy.2020.119524.

[9] Skiba AW, Wabel TM, Carter CD, Hammack SD, Temme JE, Driscoll JF. Premixed flames subjected to extreme levels of turbulence part I: Flame structure and a new measured regime diagram. Combust Flame 2018;189:407–32. http://dx.doi.org/10.1016/j.combustflame.2017.08.016.

[10] Savre J, Carlsson H, Bai XS. Tubulent methane/air premixed flame structure at high karlovitz numbers. Flow Turbul Combust 2013;90:325–41. http://dx.doi.org/10.1007/s10494-012-9426-8.

[11] Lewandowski MT. Development of turbulent combustion models in MILD regime (Ph.D. thesis), Gdánsk: Institute of Fluid Flow Machinery, Polish Academy of Science; 2018.

[12] Li P, Wang F, Mi J, Dally BB, Mei Z. MILD combustion under different premixing patterns and characteristics of the reaction regime. Energy Fuels 2014;28(3):2211–26. http://dx.doi.org/10.1021/ef402357t.

[13] Minamoto Y, Swaminathan N, Cant SR, Leung T. Morphological and statistical features of reaction zones in MILD and premixed combustion. Combust Flame 2014;161(11):2801–14. http://dx.doi.org/10.1016/j.combustflame.2014.04.018.

[14] Minamoto Y, Swaminathan N, Cant RS, Leung T. Reaction zones and their structure in MILD combustion. Combust Sci Technol 2014;186(8):1075–96. http://dx.doi.org/10.1080/00102202.2014.902814.

[15] Sorrentino G, Sabia P, de Joannon M, Cavaliere A, Ragucci R. The effect of diluent on the sustainability of MILD combustion in a cyclonic burner. Flow Turbul Combust 2016;96:449–68. http://dx.doi.org/10.1007/s10494-015-9668-3.

[16] Ertesvåg IS. Turbulent strøyming og forbrenning. Trondheim, Norway: Tapir Academic Publisher; 2000, (English version: Turbulent flow and combustion, 2008, unpublished).

[17] Ertesvåg IS, Magnussen BF. The Eddy Dissipation turbulence energy cascade model. Combust Sci Technol 2000;159:213–36. http://dx.doi.org/10.1080/00102200008935784.

[18] Magnussen BF. Modeling of NOx and soot formation by the Eddy Dissipation Concept. In: Int. flame research foundation, 1st topic oriented technical meeting. 17-19 Oct. 1989. Amsterdam, Holland; 1989.

[19] Perot JB, de Bruyn Kops SM. Modeling turbulent dissipation at low and moderate Reynolds numbers. J Turbul 2006;7:1–14. http://dx.doi.org/10.1080/14685240600907310.

[20] Gran IR, Magnussen BF. A numerical study of a bluff-body stabilized diffusion flame. Part 2. Influence of combustion modeling and finite-rate chemistry. Combust Sci Technol 1996;119:191–217. http://dx.doi.org/10.1080/00102209608951999.

[21] Magnussen BF. The Eddy Dissipation Concept – A bridge between science and technology. In: ECCOMAS thematic conference on computational combustion, 21-24 June 2005. Lisbon, Portugual; 2005.

[22] Lewandowski MT, Ertesvåg IS. Analysis of the Eddy Dissipation Concept formulation for MILD combustion modelling. Fuel 2018;224:687–700. http://dx.doi.org/10.1016/j.fuel.2018.03.110.

[23] Myhrvold T. Combustion modeling in turbulent boundary-layer flows (Ph.D. thesis), Trondheim: Norwegian University of Science and Technology; 2003, URL hdl.handle.net/11250/2577865, Dr.Ing. thesis 2003:38.

[24] Ansys Inc. Ansys fluent theory guide, Release 17.0. 2016.

[25] Ansys Inc. Ansys fluent user's guide, Release 17.0. 2016.

[26] Launder BE, Spalding DB. The numerical computation of turbulent flows. Comput Methods Appl Mech Eng 1974;3:269–89. http://dx.doi.org/10.1016/0045-7825(74)90029-2.

[27] Saffman PG, Wilcox DC. Turbulence-model predictions for turbulent boundary layers. AIAA J 1974;12:541–6. http://dx.doi.org/10.2514/3.49282.

[28] Wilcox DC. Reassessment of the scale-determining equation for advanced turbulence models. AIAA J 1988;26:1299–310. http://dx.doi.org/10.2514/3.10041.

[29] Launder BE, Sharma BI. Application of the energy-dissipation model of turbulence to the calculation of flow near a spinning disc. Lett Heat Mass Transf 1974;1:131–8. http://dx.doi.org/10.1016/0094-4548(74)90150-7.

[30] De A, Oldenhof E, Sathiah P, Roekaerts D. Numerical simulation of Delft-jet-in-hot-coflow (DJHC) flames using the Eddy Dissipation Concept model for turbulence-chemistry interaction. Flow Turbul Combust 2011;87:537–67. http://dx.doi.org/10.1007/s10494-011-9337-0.

[31] Durbin PA. Near-wall turbulence closure modeling without "damping functions". Theor Comput Fluid Dyn 1991;3:1–13. http://dx.doi.org/10.1007/BF00271513.

[32] Huang X. Measurements and model development for flameless combustion in a lab-scale furnace (Ph.D. thesis), Delft University of Technology; 2018.

[33] Rebola A, Costa M, Coelho PJ. Experimental evaluation of the performance of a flameless combustor. Appl Therm Eng 2013;50(1):805–15. http://dx.doi.org/10.1016/j.applthermaleng.2012.07.027.

[34] Rebola A, Coelho PJ, Costa M. Assessment of the performance of several turbulence and combustion models in the numerical simulation of a flameless combustor. Combust Sci Technol 2013;185(4):600–26. http://dx.doi.org/10.1080/00102202.2012.739222.